

On the design of numerical filters

A. ZEJELI (*)

Ricevuto il 13 Settembre 1971

SUMMARY. — The main object of this paper is to present some practical considerations concerning the economical approximation of ideal lowpass, highpass and bandpass filters. In some extent it is a reflection to the paper published in *Annali di Geofisica*, vol. XX, 4 by M. Galli and P. Randi: "On the design of the optimum numerical filters with a prefixed response". Some critical remarks are given on some points of their otherwise interesting and valuable work. A better solution is proposed for designing frequency filters. The purpose is to achieve good quality filtering with short operators. When using a finite length operator the frequency response is distorted. We try to minimize this effect by the application of suitably chosen truncating functions or "time windows". Some results are presented on the investigations of truncating functions. Some proposed weighting functions and transfer functions are also shown.

RIASSUNTO. — Scopo principale di questa nota è quello di illustrare alcune considerazioni pratiche circa l'approssimazione ottimale di filtri ideali passa-basso, passa-alto e passa-banda. In un certo qual modo è una risposta alla nota di M. Galli e P. Randi « On the design of the optimum numerical filters with a prefixed response » pubblicata nel Vol. XX, 4, degli « Annali di Geofisica ». Osservazioni critiche vengono fatte su alcuni punti del lavoro, comunque interessante e valido. Si propone una soluzione migliore per la progettazione di filtri di frequenza. Lo scopo è di raggiungere una buona qualità di filtraggio con operatori brevi. L'uso di un operatore di lunghezza finita, porta ad una risposta di frequenza distorta. Si tenta quindi di rendere minimo questo effetto applicando funzioni di troncamento (« time windows ») opportunamente scelte. Si portano a conoscenza alcuni risultati sulla ricerca di funzioni di troncamento, illustrando inoltre le funzioni di peso e di trasferimento proposte.

(*) Hungarian Oil and Gas Trust, Geophysical Exploration Co., Budapest (Hungary).

METHOD BY GALLI AND RANDI.

In the following the method proposed by Galli and Randi⁽²⁾ is briefly summarized. Let $S_o(f)$ be the ideal transfer function. The aim is to determine a $\{g_t\}_{t=-N}^N$ operator $2N+1$ points in such a way that its $S(f)$ transfer function should be to $S_o(f)$ as close as possible. The "distance" of the functions is measured by the root mean square deviation. Moreover be:

$$\sum_{t=-N}^N g_t = C \quad [1]$$

where, C is a constant set by us. The reason for its application is to assure that $S(0) = C$. The procedure sometimes is referred to as normalization.

Let us take an arbitrary $\{g_t\}_{t=-N}^N$ set of data. Figure 1 is to show a method for the determination of response function.

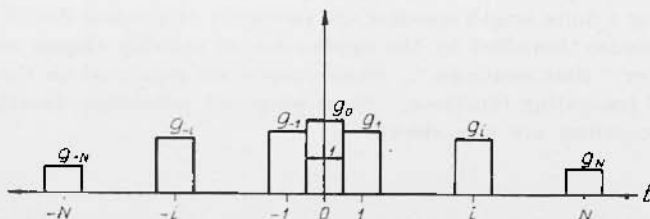


Fig. 1 - The "staircase function" method for the determination of the response function.

The Fourier transform of the staircase function shown on Figure 1 can be determined through the Fourier transform of rectangle and the shift-theorem of the Fourier transformation:

$$S(f) = \sum_{K=-N}^N g_K \frac{\sin 2\pi f \left(K + \frac{1}{2}\right) - \sin 2\pi f \left(K - \frac{1}{2}\right)}{2\pi f} \quad [2]$$

The determination of the $\{g_t\}_{t=-N}^N$ values, taking into consideration the constraint $S(0) = 1$, as well, can be performed by the Lagrange method. The following $2N+2$ sets of equations have to be solved:

$$\frac{\partial}{\partial g_i} \left\{ F(g_{-N} \dots g_N) + \lambda f(g_{-N} \dots g_N C) \right\} = 0 \quad [3]$$

$$f(g_{-N} \dots g_N) = 0 \quad i = -N \dots 0 \dots N$$

where

$$F(g_{-N} \dots g_N) = \int_{(f)} [S_o(f) - S(f)]^2 df \quad [4]$$

$$f(g_{-N} \dots g_N) = \sum_{i=-N}^N g_i - C = 0. \quad [5]$$

The general solution is

$$g_K = 2 [\gamma_{K+1/2} - \gamma_{K-1/2} - \gamma_{N+1/2}/(N + 1/2)] + C/(2N + 1) \quad [6]$$

where

$$\gamma_K = \int_{(f)} S_o(f) \frac{\sin 2\pi f K}{2\pi f} df. \quad [7]$$

INVESTIGATION.

The frequency response given in equation [2] does not correctly represent the filter characteristics of the $\{g_i\}_{i=-N}^N$ operator. Eq. [2] is the Fourier transform of a staircase function and its only relation with the set of data is that its values at some arguments i ($i = -N \dots N$) correspond to g_i . With the same justification many other type of functions could be applied. An example is shown in Figure 2.

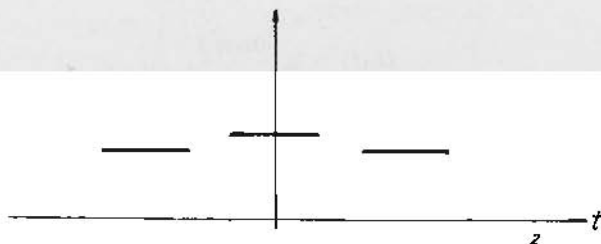


Fig. 2 -- The determination of the response function in the case of $0 < a < 1/2$.

It is evident that in case of $a = 0$ one gets the staircase function back, in case of $a = 1/2$ the approximation is done with a series of

triangles. The Fourier transform of a triangle of unit base and unit height is

$$H(f) = \frac{1}{2} \frac{\sin^2 \frac{\pi}{2} f}{\left(\frac{\pi}{2} f\right)^2}. \quad [8]$$

Using this relation and applying the shift-theorem one gets

$$S_1(f) = \sum_{i=-N}^N g_i \frac{\sin^2 \frac{\pi}{2} f}{\left(\frac{\pi}{2} f\right)^2} \cos 2\pi f i \quad [9]$$

for the transfer function instead of that given by Eq. [2]. It should be noted that in formulas [2] and [9] $g_i = g_{-i}$ was assumed which assures zero phase shift. The Fourier transform of the operator can easily be computed for any a ($0 \leq a \leq \frac{1}{2}$) value if one recognizes the fact that a trapezoid is the convolution of two rectangles. This way the Fourier transform of a trapezoid will be the product of the transform of two rectangles. By the choosing various a values infinite number of response functions can be assigned to the weighting function $\{g_i\}_{i=-N}^N$ and the optimum will be selected from functions fixed in $a = a_0$.

Although the reasons given so far are good enough to prove our stand, still we are putting forward a simple example to show that incorrect results can be received by the selection of $a = 0$ given in the cited author's paper.

If a set of data to be filtered is convolved by an arbitrary value based on formula [2] at $N = 0$:

$$G_o(f) = g_o \frac{\sin \pi f}{\pi f}. \quad [10]$$

According to the formula the spectrum of the filtered data set will deviate from the original one and e. g. $f = \frac{K}{T}$ frequencies will disappear from it ($K = 1, 2 \dots$). If a set of data is convolved by a constant the result is the product of all values by this constant. Thus the spectrum of set of filtered data will correspond to the original one allowing for a uniform change in the energy level of individual frequencies. The spectrum will be enlarged or reduced by a^2 depending on $a \leq 1$ value. Neither the energy proportion of individual frequencies

"proportion of weight" will change, nor will its "shape" be altered in the time domain.

A correct relation between the $\{g_i\}_{i=-N}^N$ operator and its transfer function is supplied by the numerical Fourier transformation:

$$A(f) = \sum_{i=-N}^N g_i e^{-j2\pi f i} = g_0 + 2 \sum_{i=1}^N \cos 2\pi f i \quad [11]$$

by assuming symmetrical set of g_i coefficients and unit sampling interval. Referring to the above example [11]:

$$A_0(f) = g_0 \quad [12]$$

and this is a correct result. If we want to follow Galli and Randi's method ⁽²⁾ Eq. [3] should be solved, but instead of Eq. [2], Eq. [11] should be substituted. Eq. [3] will then give:

$$\begin{aligned} \frac{\partial}{\partial g_i} \left\{ \int_0^1 \left[S_0(f) - \sum_{i=-N}^N g_i e^{-j2\pi f i} \right]^2 df + \lambda \sum_{i=-N}^N g_i - \lambda C \right\} = \\ = -2 \int_0^1 \left[S_0(f) - \sum_{i=-N}^N g_i e^{-j2\pi f i} \right] e^{-j2\pi f i} df + \lambda, \quad i = 0, 1 \dots N. \end{aligned} \quad [13]$$

If $S_0(f)$ is symmetrical with respect to the origin:

$$S_i = \int_0^1 S_0(f) e^{-j2\pi f i} df. \quad [14]$$

On the other hand supposing that the set of g_i values is also symmetrical:

$$g_i = \int_0^1 \left| \sum_{i=-N}^N g_i e^{-j2\pi f i} \right| e^{j2\pi f i} df \quad [15]$$

and introducing the notion $\mu = \frac{\lambda}{2}$ Eq. [13] will be:

$$g_i - s_i + \mu = 0 \quad i = -N \dots 0 \dots N. \quad [16]$$

Summarizing all Equations from $i = -N$ up to $i = N$ and taking into consideration Eq. [5] we obtain:

$$C - \sum_{i=-N}^N s_i + (2N + 1)\mu = 0. \quad [17]$$

From this Eq.:

$$\mu = \frac{\sum_{i=-N}^N s_i - C}{2N + 1} \quad [18]$$

thus:

$$g_i = s_i - \mu = s_i + \frac{C - \sum_{i=-N}^N s_i}{2N + 1} \quad i = -N \dots N. \quad [19]$$

According to Eq. [19] the g_i coefficients can be computed by taking the inverse Fourier transform of the ideal transfer function $S_0(f)$. The result is sampled at $i = -N \dots 0 \dots N$ and the resulting $\{s_i\}_{i=-N}^N$ operator plus constant is normalized by making sure that the sum of the coefficients be a constant C prescribed before.

The cardinal point in the procedure is that an infinite long weighting function is computed then this function is truncated by a $2N+1$ points long rectangle "time window" and at last the transfer function belonging to the truncated data set — Eq. [11] — is modified to yield prefixed value at zero frequency. In case of low pass filters $C = 1$, high pass and band pass filters $C = 0$ are usually applied.

Since the weighting functions belonging to the ideal transfer functions for the above mentioned filters are known, or can easily be determined analytically solution of Eq. [13] becomes unnecessary. The results of Eq. [19] can be obtained in a shorter way through the use of Rayleigh's theorem and post normalization. It is known (1) that if the Fourier transform of an $h(t)$ function is $H(f)$ then:

$$\int_{(f)} H(f)^2 df = \int_{(t)} h^2(t) dt. \quad [20]$$

Using this relation we can write:

$$\int_{(f)} \left\{ S_0(f) - A(f) \right\}^2 df = \sum_{-\infty}^{+\infty} (g_i - s_i)^2 = \sum_{-\infty}^{-i-1} s_i^2 + \quad [21]$$

$$+ \sum_{-N}^N (g_i - s_i)^2 + \sum_{N+1}^{\infty} s_i^2.$$

The minimum is reached when the g_i values are chosen in such a way

that the r.m.s. deviation will be minimum. Only the middle sum depends on the selection of g_i values. Since all sums are positive or zero the righthand side will be minimum if $s_i = g_i$ for all i value.

In the root mean square sense the rectangle time-window of $2N+1$ points length assures the optimum. Normalization can be carried out after truncation. If the sum of coefficients should be C i.e.:

$$\sum_{i=-N}^N \bar{g}_i = \sum_{i=-N}^N (s_i + \mu) = C \quad [22]$$

the normalization factor is:

$$\mu = \frac{C - \sum_{i=-N}^N s_i}{2N + 1} \quad [23]$$

thus:

$$\bar{g}_i = s_i + \frac{C - \sum_{i=-N}^N s_i}{2N + 1} \quad [24]$$

The result here corresponds to Eq. [17].

This type of normalization is not advantageous. Since the transfer function of the normalized coefficients is given by:

$$\begin{aligned} G(f)_{\text{norm}} &= \sum_{i=-N}^N (g_i + \mu) e^{-j2\pi fi} = \sum_{i=-N}^N g_i e^{-j2\pi fi} + \mu \sum_{i=-N}^N e^{-j2\pi fi} = \\ &= G(f) + \mu \frac{\sin(2N+1)\pi f}{\sin \pi f} \end{aligned} \quad [25]$$

The spectrum associated with the unnormalized data set is distorted by the second in the sum [25]. Curve in Figure 3 represents the transfer function of unnormalized low pass filter, curve *a* in Figure 4 represents the normalizing function, curve *b* in Figure 4 is the normalized transfer function. Comparing curve *b* in Figure 4 to curve *a* in Figure 3 the distortion mentioned above can be well noticed.

Simultaneous modification of all coefficients according to the formula

$$g_i = \frac{g_i}{\sum_{i=-N}^N g_i} \quad i = -N \dots N \quad [26]$$

gives better results. This way $\sum_{-N}^N g_i = 1$ is assured, but the shape of the transfer function will not be distorted. Curve *b* of Figure 3 was normalized this way. The vertical scale of this curve is magnified by a factor of 10.

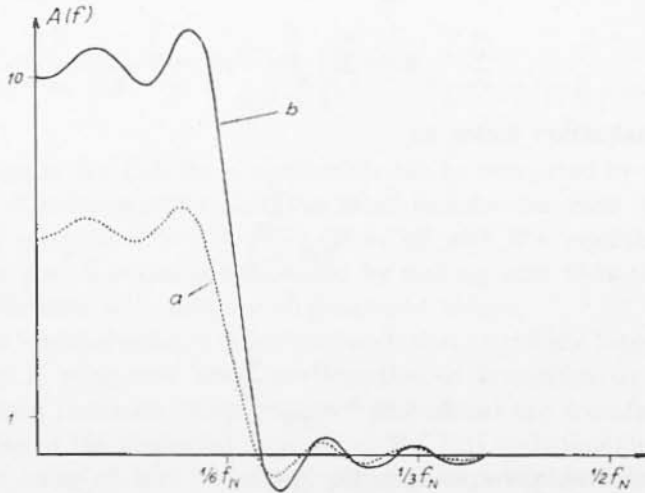


Fig. 3 - Curve *a* represents the transfer function of an unnormalized low pass filter.

Curve *b* represents the normalized transfer function using Eq. [26].

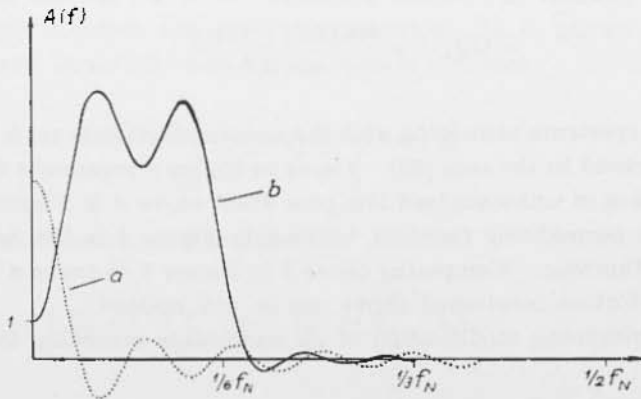


Fig. 4 - Curve *a* represents the normalized transfer function using Eq. [19] or Eq. [24].

Curve *b* represents the normalizing function.

DESIGN OF FREQUENCY FILTERS AND IMPROVEMENT OF THEIR TRANSFER CHARACTERISTICS BY TRUNCATING FUNCTIONS.

Let us assume that we are given some transfer function of a normalized low pass filter $A_l(f, f_0)$ and the corresponding $\{s_{l,i}\}_{i=-N}^N$ weighting function. The cut-off frequency is denoted by f_0 . The transfer function and weighting function of a high pass filter with identical cut-off frequency can be derived from the given low pass filter.

The transfer function of the high pass filter is:

$$A_h(f, f_0) = 1 - A_l(f, f_0) \quad [27]$$

and the weighting function:

$$\begin{aligned} s_{o,h} &= 1 - s_{o,l} \\ s_{l,h} &= -s_{l,l} \quad i = \pm 1 \dots \pm N. \end{aligned} \quad [28]$$

A filter that passes the frequency band (f_1, f_2) can be determined from two low pass filters with cut-off frequencies f_1 and f_2 . Let be $f_1 < f_2$. In this case the transfer function of the band pass filter will be:

$$A_b(f, f_1, f_2) = A_l(f, f_2) - A_l(f, f_1) \quad [29]$$

and its weighting function is:

$$s_{l,b} = s_{l,l_2} - s_{l,l_1} \quad i = 0, \pm 1 \dots \pm N. \quad [30]$$

Finally, if one wants to design a band reject filter, which eliminates the frequency band (f_1, f_2) , the transfer function will be:

$$A_r(f, f_1, f_2) = 1 + A_l(f, f_1) - A_l(f, f_2) \quad [31]$$

and its weighting function is:

$$\begin{aligned} s_{o,r} &= 1 + s_{o,l_2} - s_{o,l_1} \\ s_{l,r} &= s_{l,l_2} - s_{l,l_1} \quad i = \pm 1 \dots \pm N. \end{aligned} \quad [32]$$

Two observations can be made. If the high cut filters have been normalized, the derived filters will automatically be normalized, no extra effort is needed. In other words the derived filters inherit the beneficial or ill properties of the high cut filters. If the transfer function of a high cut filter has been smooth and its steepness has been appropriately chosen, filters derived from it will hold the same properties.

For this reason it is quite sufficient to deal with the improving of the transfer properties of the high cut filters.

Observing transfer function a on Figure 3 positive and negative overshoots can be noticed in the neighbourhood of the cut-off frequency. This results in the enhancement of certain low frequencies. Moreover, in the negative overshoot domain phase reversal occurs. This is known as the Gibbs phenomenon (¹). It is our intention to eliminate or minimize these undesirable distortions by using the same or shorter weighting functions.

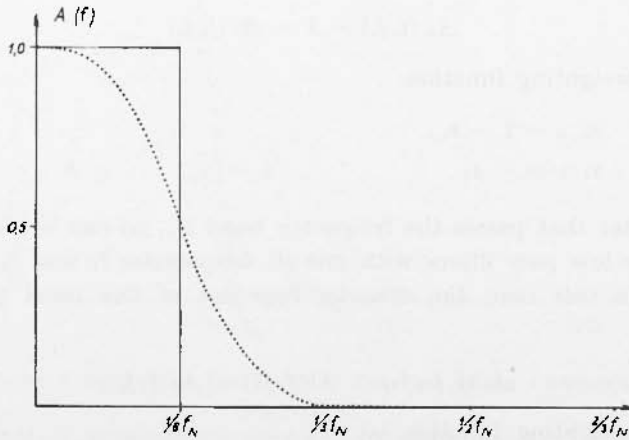


Fig. 5 - The transfer function of a low pass filter. The applied truncating functions is $f_i(i:K)$. The cut-off frequency is $f = 1/6 f_N$; $K = 0.02$, $N = 10$.

Let us denote the desired truncating function with $u(t)$. $u(t)$ must be an even function in order to reserve the zero phase shift property of the original filter. Moreover, outside of the $\left(-\frac{T}{2}; +\frac{T}{2}\right)$ interval it must be either zero or at least negligibly small. In the time domain the truncation can be described by:

$$\bar{s}(t) = s(t) \cdot u(t) \quad [33]$$

and the relation of the spectra of the original and truncated weighting function is:

$$\bar{S}(f) = S(f) \star u(f) \quad [34]$$

It is known that:

$$S(f) = S(f) \star \delta(f) \quad [35]$$

where $\delta(f)$ is the Dirac- δ function. The better is the Dirac-impulse approximated by the $U(f)$ - i.e. the Fourier transform of $u(t)$ - the less noticeable the influence of truncation. Thus, the spectrum of the truncating function should concentrate into the neighbourhood of the origin as close as possible. Reminding that short weighting function can be derived only rapidly decreasing truncating function and referring to the similarity theorem of the Fourier transformation which states that contraction in one domain corresponds to expansion in the other domain we may conclude that the two requirements contradict each other. What we are seeking is the best compromise between the two requirements. The aim will be to find functions which decrease rapidly enough in both domains.

SELECTION OF TRUNCATION FUNCTIONS ON THE BASIS OF ENERGY CONCENTRATIONS.

Let us define the x energy bandwidth by the following formula:

$$\int_{-\frac{x}{2}}^{+\frac{x}{2}} u^2(t) dt = \eta \int_{-\infty}^{+\infty} u^2(t) dt \quad [36]$$

where:

$$0 \leq \eta \leq 1$$

$x = x(\eta)$ values will be referred to as the η -level bandwidth of $u(t)$ in the time domain. Formula [36] shows that 100 η percent of total energy of $u(t)$ concentrates into the $-\frac{x}{2}$; $+\frac{x}{2}$ interval.

The energy concentration in the frequency domain can be measured in a similar way thus, the bandwidth in the frequency domain can be defined as:

$$\int_{-\frac{y}{2}}^{+\frac{y}{2}} u^2(f) df = \eta \int_{-\infty}^{+\infty} u^2(f) df, \quad [37]$$

It should be noted that we shall investigate symmetrical functions which Fourier transforms will be real thus, the application of the absolute value is superfluous in the above formula. The product of the two bandwidths:

$$\Omega(\eta) = x(\eta) \cdot y(\eta) \quad [38]$$

will be called the "composite bandwidth" of the $u(t)$ function. The smaller is this product at some η — level the stronger is the energy concentration in both domains. Thus the $\Omega(\eta)$ could serve as a design criterion for the truncating function. The following functions have been investigated.

Table 1 — BANDWIDTHS IN THE TWO DOMAINS AND THE COMPOSITE BANDWIDTHS

	x_1	y_1	x_2	y_2	x_3	y_3	$x_1 \cdot y_1$ $\eta = 0,71$	$x_2 \cdot y_2$ $\eta = 0,9$	$x_3 \cdot y_3$ $\eta = 0,99$
$e^{-\pi t^2}$	0,58	0,58	0,92	0,92	1,44	1,44	0,34	0,85	2,08
$e^{- t }$	1,22	0,22	2,3	0,42	4,6	1,06	0,27	0,97	4,86
$\frac{1}{10} \begin{matrix} 1 & \text{if } t < 0,4 \\ (0,5-t) & \text{if } 0,4 < t < 0,5 \\ 0 & \text{if } t > 0,5 \end{matrix}$	0,6	0,86	0,76	1,34	0,88	3,76	0,52	1,02	3,31
$\frac{1}{0} \begin{matrix} 1 & \text{if } t < 0,5 \\ 0 & \text{if } t > 0 \end{matrix}$	0,7	0,84	0,9	1,6	0,99	15,1	0,59	1,44	14,8
$\frac{1-2 t }{0} \begin{matrix} 1-2 t & \text{if } t < 0,5 \\ 0 & \text{if } t > 0,5 \end{matrix}$	0,34	1,11	0,54	1,68	0,78	2,60	0,38	0,91	2,04
$e^{- t } \frac{\sin t}{t}$	1,0	0,3	1,78	0,5	3,18	3,14	0,30	0,89	3,64
$e^{- t } \cos \pi t$	1,32	1,1	2,14	1,3	4,3	1,9	1,45	2,79	8,15
$\frac{\cos \pi t}{0} \begin{matrix} \text{if } t < 0,5 \\ \text{if } t > 0,5 \end{matrix}$	0,4	1,02	0,58	1,54	0,8	2,36	0,41	0,83	1,89
$\frac{0,5 + 0,5 \cos \pi t}{0} \begin{matrix} \text{if } t \leq 1 \\ \text{if } t > 1 \end{matrix}$	0,62	0,80	0,93	1,28	1,36	5,64	0,50	1,20	7,65
$\frac{0,54 + 0,46 \cos \pi t}{0} \begin{matrix} \text{if } t \leq 1 \\ \text{if } t > 1 \end{matrix}$	0,66	0,86	1,00	1,35	1,52	7,21	0,57	1,35	10,8

Time windows:

$$u_1(t) = e^{-\pi t^2}$$

$$u_2(t) = e^{-|t|}$$

$$u_3(t) = \begin{cases} 1 & \text{if } |t| \leq 0,4 \\ 10(0,5 - t) & \text{if } 0,4 < |t| \leq 0,5 \\ 0 & \text{if } |t| > 0,5 \end{cases}$$

$$u_4(t) = \begin{cases} 1 & \text{if } |t| \leq 0,5 \\ 0 & \text{if } |t| > 0,5 \end{cases}$$

$$u_5(t) = \begin{cases} 1 - 2t & \text{if } |t| \leq 0,5 \\ 0 & \text{if } |t| > 0,5 \end{cases}$$

$$u_6(t) = e^{-|t|} \frac{\sin t}{t}$$

$$u_7(t) = e^{-|t|} \cos \pi t$$

$$u_8(t) = \begin{cases} \cos \pi t & \text{if } |t| \leq 0,5 \\ 0 & \text{if } |t| > 0,5 \end{cases}$$

$$u_9(t) = \begin{cases} 0,5 + 0,5 \cos \pi t & \text{if } |t| \leq 1 \\ 0 & \text{if } |t| > 1 \end{cases}$$

$$u_{10}(t) = \begin{cases} 0,54 + 0,46 \cos \pi t & \text{if } |t| \leq 1 \\ 0 & \text{if } |t| > 1 \end{cases}$$

Frequency windows:

Gaussian $u_1(f) = e^{-\pi f^2}$

exponential $u_2(f) = \frac{2}{1 + (2\pi f)^2}$

Ormsby $u_3(f) = \text{sinc}^*(*) (0,2f) \text{sinc} (0,9f)$

rectangle $u_4(f) = \text{sinc } f$

triangle $u_5(f) = \text{sinc}^2 \frac{f}{2}$

modified exponential $u_6(f) = \text{arc tg } \frac{1}{2} (\pi f)^2$

modified exponential $u_7(f) = \frac{1}{1 + 4 \pi^2 (f + 0,5)^2} - \frac{1}{1 + 4 \pi^2 (f - 0,5)^2}$

cosine $u_8(f) = \text{sinc} (f + 0,5) + \text{sinc} (f - 0,5)$

Hamming $u_9(f) = 0,5 \text{sinc } f + 0,25 \text{sinc} (f - 1/2) + 0,25 \text{sinc} (f + 1/2)$

Hamming $u_{10}(f) = 0,54 \text{sinc } f + 0,23 \text{sinc} (f - 1/2) + 0,23 \text{sinc} (f + 1/2)$

(*) sinc is an abbreviation of sinus cardin alis.

The functions having the same subscript are essentially Fourier transform pairs. Some constant factors were omitted because of neither definition [36] or [37] are "sensitive" to a constant multiplier. Several of the investigated functions are well known from the literature. Bandwidths in the two domains and the composite bandwidths are

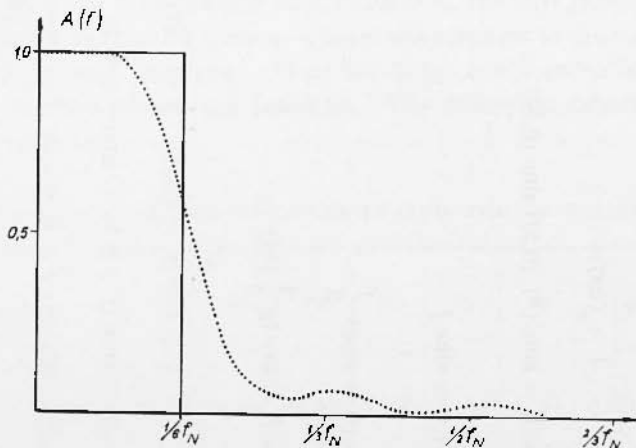


Fig. 6 - The transfer function of a low pass filter. The applied truncating function is $f_2(i; K)$. The cut-off frequency is $f = 1/6 f_N$; $K = 0.1$, $N = 10$.

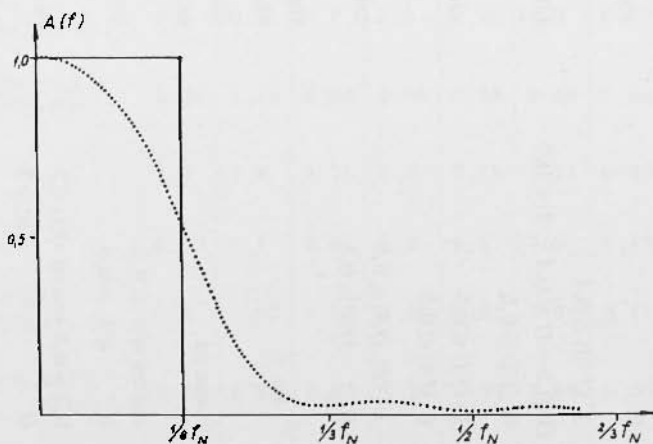


Fig. 7 - The transfer function of a low pass filter. The applied truncating function is $f_3(i; K)$. The cut-off frequency is $f = 1/6 f_N$; $K = 10$, $N = 10$.

shown in Table 1. Three η — levels were selected. These are $\eta = \frac{1}{\sqrt{2}}$; 0,9; 0,99. As it is seen from the table the “ best ” truncating function

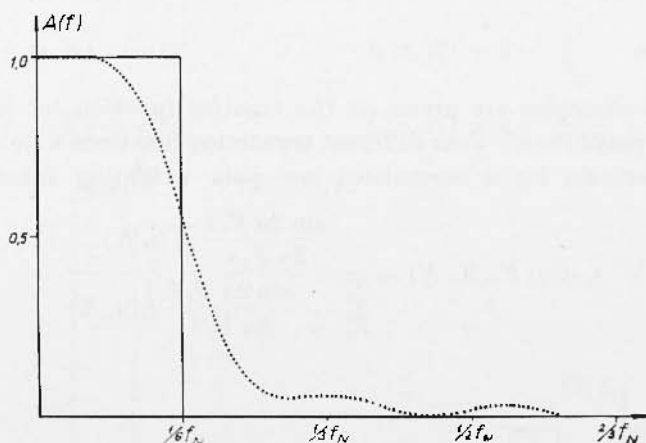


Fig. 8 — The transfer function of a low pass filter. The applied truncating function is $f_0(i; K)$. The cut-off frequency is $f = 1/6 f_N$; $K = 0.0945$, $N = 10$.

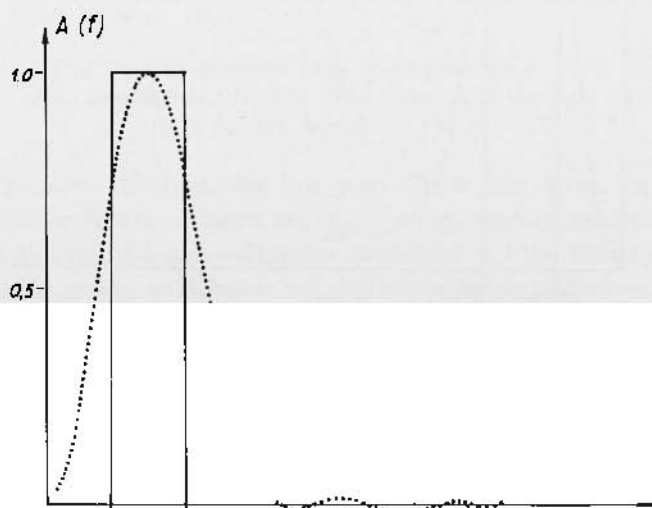


Fig. 9 — The transfer function of a band pass filter. The applied truncating function is $f_1(i; K)$. The pass band is the interval $(1/18 f_N; 1/9 f_N)$; $K = 0.05569$, $N = 17$.

cannot be unambiguously determined because different functions possess the minimum composite bandwidths at different levels. The truncating functions u_1 , u_2 , u_3 and u_6 , however are better.

EXAMPLES.

Some examples are given on the transfer function for low pass and band pass filters. Four different truncating functions were applied. General formula for a normalized low pass weighting function is:

$$s_1(i, j, F_o, K, N) = \frac{\frac{\sin 2\pi F_o i}{2\pi F_o i} f_j(i, K)}{\sum_{i=-N}^N \frac{\sin 2\pi F_o i}{2\pi F_o i} f_j(i, K)} \quad [39]$$

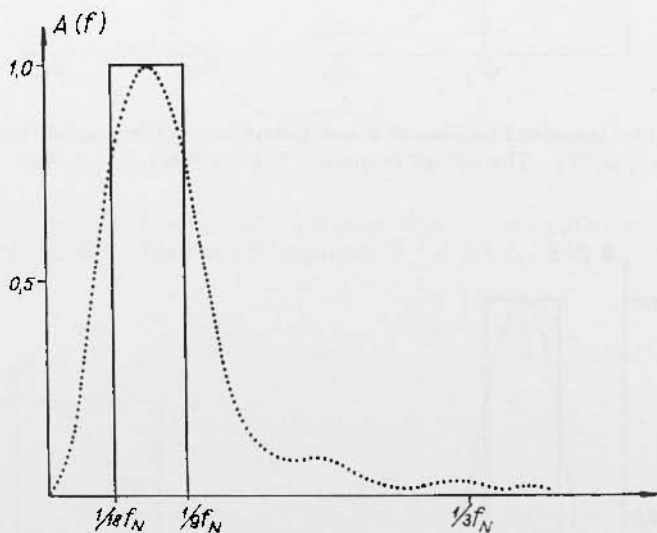


Fig. 10 - The transfer function of a band pass filter. The applied truncating function is $f_2(i; K)$. The interval of the pass band is $(1/18 f_N; 1/9 f_N)$; $K = 0.0847$, $N = 17$.

where:

N determines the length of the weighting function as $(2N + 1)$

F_o cut-off frequency in relative frequencies

$$\left(0 < F_o < \frac{1}{2} - F_{N_{\text{youtst}}} \right)$$

- j type of truncating function
- K parameter of truncating function.

Truncating functions used:

$$\begin{aligned}
 f_1(i, K) &= e^{-Ki^2} & f_3(i, K) &= 1 - \frac{|i|}{K} \\
 f_2(i, K) &= e^{-K|i|} & f_4(i, K) &= e^{-|i|K} \frac{\sin K \cdot i}{K \cdot i}
 \end{aligned}
 \tag{40}$$

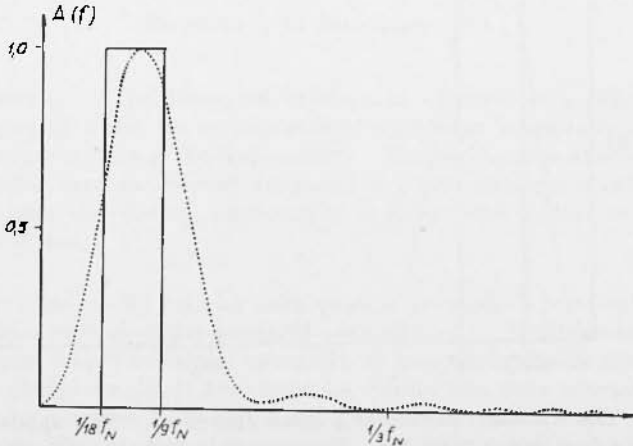


Fig. 11 - The transfer function of a band pass filter. The applied truncating function is $f_4(i; K)$. The interval of the pass band is $(1/18 f_N; 1/9 f_N)$; $K = 17, N = 17$.

Some transfer functions for low pass filters are shown on Figs. 5-8. The transfer function shown on Fig. 5 is very smooth especially favourable in the reject band. Transfer functions of Figs. 6 and 8 are more favourable in the pass band. If better plate is needed — and some secondary maximums are allowed for in the reject band — the use of the latter is recommended.

On Figs. 9-12 pass band filters are shown. The same truncating functions were used as above. General formula is as follows:

$$s_b(i, F_1, F_2, K, N) = \frac{\frac{\sin 2\pi F_2 i}{2\pi F_2 i} f_j(i, K)}{\sum_{-N}^N \frac{\sin 2\pi F_2 i}{2\pi F_2 i} f_j(i, K)} - \frac{\frac{\sin 2\pi F_1 i}{2\pi F_1 i} f_j(i, K)}{\sum_{-N}^N \frac{\sin 2\pi F_1 i}{2\pi F_1 i} f_j(i, K)} \tag{41}$$

F_2 and F_1 are the high and low sides of the pass band in relative fre-

quencies thus, $0 < F_1 < F_0 < \frac{1}{2}$. On the basis of the transfer functions the various truncating functions can also be compared because the operators were of the same length. Truncating function $f_1(i, K)$ seems to be the most favourable.

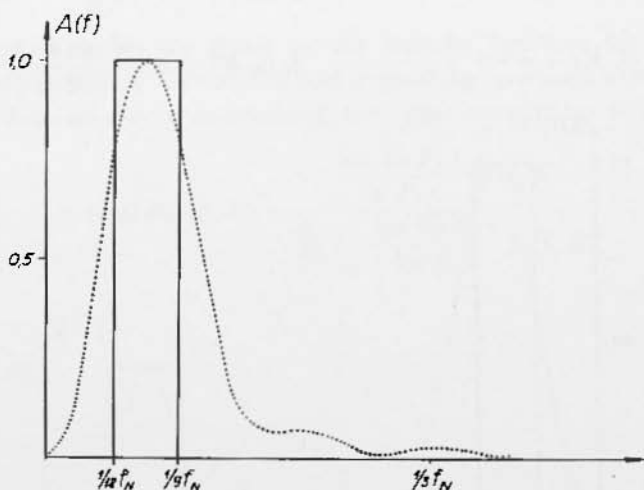


Fig. 12 - The transfer function of a band pass filter. The applied truncating function is $f_A(i; K)$. The interval of the pass band is $(1/18 f_N; 1/9 f_N)$; $K = 0.07682$, $N = 17$.

ACKNOWLEDGEMENT.

The author is greatly indebted to the Geophysical Exploration Co. of the Hungarian Oil & Gas Trust for its permission to publish this paper and to *Dr. Attila Mcsko* of Roland Eötvös University for many of his suggestions and encouraging remarks on the subject.

REFERENCES

- (1) BRACEWELL R., *The Fourier Transform and its Applications*. New York, McGraw-Hill Book Co., 1965.
- (2) GALLI M. and RANDI P., *On the Design of the Optimum Numerical Filters With a Prefixed Response*. "Annali di Geofisica", XX, 4, 1967.

The Karnaveh (Northeast Iran) earthquake of 30 July, 1970

N. N. AMBRASEYS (*) - A. A. MOINFAR (**) - J. S. TCHALENKO (*)

Ricevuto il 15 Settembre 1971

SUMMARY. — The Karnaveh earthquake occurred in a relatively quiescent region in which no earthquakes of significant magnitude are known to have occurred during the last century. The earthquake affected a sparsely populated area and caused comparatively little damage; it caused large-scale slumping and sliding, particularly in steep-sided valleys of loess and recent sediments.

RIASSUNTO. — La regione nella quale è avvenuto il terremoto di Karnaveh, è una regione — dal punto di vista sismico — relativamente quieta. Non si hanno infatti notizie di terremoti, di magnitudo significativa, occorsi in questo ultimo secolo. Il terremoto ha colpito una zona scarsamente popolata ed ha causato, in proporzione, lievi danni, provocando — però — gran numero di voragini e franamenti, particolarmente in valli scoscese formate da « loess » e sedimenti recenti.

INTRODUCTION.

The Karnaveh earthquake of 30 July 1970 occurred in north-east Iran, not far from the borders of Turkestan, Fig. 1. The shock occurred at dawn, at about 4.30 local time (00h 52m 19s GST). The epicentre of the earthquake was computed by two seismological centres with the following results: BCIS 37.9°N - 55.9°E, USCGS 37.8°N - 55.9°E. The magnitude of the shock as calculated by different stations varied between $M_s = 6.3$ and 6.7. Preliminary focal depth determinations indicated a shallow focus, less than 20 kilometres deep. The main shock was felt over an area of about 100,000 km². There were comparatively few aftershocks, all of low magnitude, which added very little to the damage caused by the main shock.

(*) Imperial College of Science and Technology, London (England).

(**) UNESCO, Plan Organization, Tehran (Iran).

The earthquake occurred in the upper reaches of the Gorgan River, in what used to be called formerly eastern Sahra-i-Turkman, a rather isolated and thinly populated area south of the River Atrek. The main shock affected an area of about 7,000 km² which is very sparsely populated, in places being almost a desert. With very few

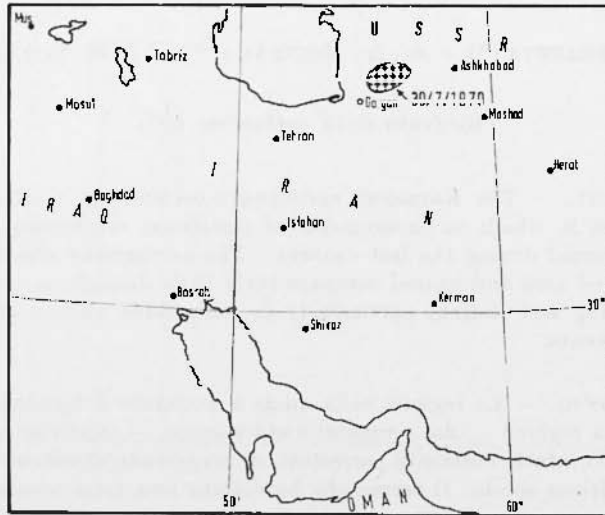


Fig. 1 - Location map of the Karnaveh earthquake of 30 July 1970.

exceptions, all houses in the epicentral region are of adobe brick or mud-wall construction with flat roofs covered with mud. There are very few properly built houses and there are no other types of man-made structures the damage of which could serve as a measure in assessing intensities. Thus, from the behaviour of local houses alone it was not possible to determine intensities greater than about VII (MM). There is some indirect evidence, however, that the maximum intensity did not exceed VIII (MM).

As the earthquake happened very early in the morning when most of the men were at dawn prayers in the open court-yards, it was mainly women and children who were killed. The exact number of people killed is not known but it is probably between 170 and 200. More than 350 people were injured and about 2,000 to 3,000 housing units were destroyed or damaged beyond repair in 40 villages and settlements. The largest settlements affected by the earthquake are those Karnaveh, Agheman, Chenaran, Gholidak Shahrak and Yemlak.

A number of smaller settlements, however, such as Baba Shamalak and Meydanjik, which are situated in the middle of a barren region, suffered greater damage.

Field work and the study of aerial photographs taken after the earthquake showed absolutely no evidence of surface faulting. Large-scale slumping and sliding was noticed in many places, particularly in steep-sided valleys incised in loess and Pliocene sediments.

THE KARNAVEH EARTHQUAKE.

The seismic history of the upper reaches of the Gorgan River (shown in inset Figg. 1-2) is very little known. In earlier days this was a flourishing district with a well recorded history. Late in the 12th century, however, like other districts near the southern shores of the Caspian Sea, it was overrun and devastated by the Mongol invasion, and again by Timur at the close of the 14th century, after which there is a significant gap in the written history of the district. As late as the middle of the 19th century, this part of Khorassan remained almost inaccessible and very little known.

The earliest earthquake in Gorgan, for which we could find written evidence, occurred in December 856 and affected the district of Jurjan, causing heavy damage at Bistam and particularly in Jurjan, Fig. 2, *Girgis al-Makin*, and *Girgis abu'l Farag*. In August 943 another earthquake ruined Nessa almost totally, killing 5,000 people; it is not certain, however, whether Nessa was the old site just south of Ashkhabad or the early town of Nisa now known as Darreh Gaz, *Abd al-Rahman*, Fig. 2. A few years later, in 985, Jurjan was damaged again, most probably by a shock caused due to a meteoritic fall rather than to an earthquake, *Abu Darr Ahmad*. This city was damaged again in 1280, *Hamd-Allah*. After that year, and for the following five and a half centuries we could find no written evidence of major earthquakes in that district.

During the 19th century, the first major earthquake occurred in 1852, on the 22nd of February, and almost totally destroyed Khabushan, modern Quehan, killing 2,000 people (23. 24). On the 20th January 1868 another earthquake caused considerable damage in the region between Shahrud and Sabzavar ruining Allhak (4. 24). On the 23rd December 1871 a major earthquake devastated the region of Khabushan killing more than 2,000 people in the district of Qu-

chan (4, 13, 15, 23, 24). The following year, on the 6th of January 1872, an equally strong earthquake caused serious damage between Bojnurd and Quchan, in which about 4,000 people were killed (13, 14, 15, 24). Bojnurd was damaged again on the 2nd of April 1879, and 700 people perished in the ruins (4, 24). A few years later, on the 28th of June 1890, a damaging earthquake ruined the district between Asterabad, Shahrud and Bostam, causing particularly heavy damage at Tash; at Bastam 150 people were killed (15, 24). The earthquake of the 17th November 1893 in Quchan affected a large area, killing 5,000 people. It was followed by many strong aftershocks which added to the damage; the aftershocks of January 1895 were particularly severe and they ruined completely Quchan (12, 15, 21, 23, 24). The earthquake of the 15th of January 1898 caused considerable damage in the region of Asterabad and at Chikishlar (24).

Destructive earthquakes continued in the present century and these have been studied by Ambraseys *et al* (3). The most important earthquakes of the 20th century for which we have sufficient macro-seismic information are the following:

On the 4th February 1923, Bojnurd suffered considerable damage and about 200 houses collapsed. On the 17th September of the same year, 30 villages in the region of Bojnurd were ruined and more than 150 people were killed. Shirvan was damaged on the 10th December 1925 and a few people were killed. A major earthquake of magnitude about 7.0 occurred in the upper reaches of the Atrek River on the 1st May 1929. The shock caused serious damage in Iran and in the Soviet Turkestan killing more than 3,500 people. The villages of Gifan, Germab, Zardau, Kheyrebad, Rabat, Jafarabad, Arsanab, Sarani, Kulun, Kurkulab, and Kheyrebad were almost totally destroyed. The damage was equally heavy in the district of Shirvan where 2,500 people were killed. Bojnurd and Quchan suffered less. Ashkhabad was badly shaken and a small number of people were injured. The damage extended to Jajarm, Bandar Gaz and Bam. This earthquake was associated with faulting which extended for 40 kilometres between Khajili and Bagham, to the east of the Quchan-Bojnurd road. Aftershocks continued for many months causing serious damage (6, 16) (Nazarevski 1932). On the 5th April 1944 an earthquake damaged one third of the houses in Gorgan, many of which collapsed, killing 20 people; a number of villages in the Gorgan district were ruined. Shirvan was damaged again on the 10th July 1947 and a number of houses collapsed. More shocks in June 1948 caused additional damage

to the district and also to the town of Shirvan; aftershocks continued for four months ruining a number of villages between Gifan and Shirvan. Late in 1952 a series of damaging earthquakes affected Goek Tepe, and in the following year, on the 18th of April, a series of shocks which lasted till June, caused some damage in Gorgan, particularly at Aliabad, where a number of houses collapsed. The earthquake of 8th December 1962 damaged houses and public buildings in Shahrud and in the following year, on the 31st of March, a number of villages in the Kuh-e Shah Jahan district were totally destroyed; at Dahneh Hodjagh a considerable number of houses collapsed and many people were killed. The damage extended to Bam and Soltanabad, and it was aggravated by aftershocks. Iraj, Meynabad and Firuzeh, villages situated at the foothills of Allah-Dagh were damaged by an earthquake on the 3rd February 1967. Two years later, on the 3rd of January, another earthquake ruined the villages of Dahneh Hodjagh, Bam and those villages belonging to the Shirvan district, killing 50 people and making 2,000 homeless (*). Nishapur, Bojnurd, Quchan, Sabzavar and Isfarayen suffered minor damage. Farseyan suffered additional damage by the shock of 25th February 1970, and a month later, on the 3rd of April, a strong earthquake caused minor damage at Gorgan.

Thus, the macroseismic evidence indicates that destructive earthquakes have been occurring either along the Elburz ranges or at their junction with the Kopet Dagh, particularly in the vicinity of Allah Dagh. This is confirmed by the distribution of epicentres, shown in Fig. 3, which shows that during the last 50 years major shocks follow the Elburz and the Kopet Dagh alignments (**).

The geology as well as the tectonics of the region shown in Fig. 3 are very little known, and the small-scale geological mapping of the region which is now available (17, 18, 20) is of little use for the purpose intended.

The area affected by the earthquake of 30th July 1970 (Fig. 3 and Fig. 4) is of comparatively low relief, extending eastwards

(*) Rezanov (18) and Rustanovich (19) mention an earthquake on the 23rd of January 1909 which they say destroyed 60 villages in Bojnurd. In fact, this earthquake occurred in Burujird and not in Bojnurd, the former being about 900 kilometres to the southwest of Bojnurd (5).

(**) Figure 3 has been prepared on the basis of data in *Ambraseys et al* (3).

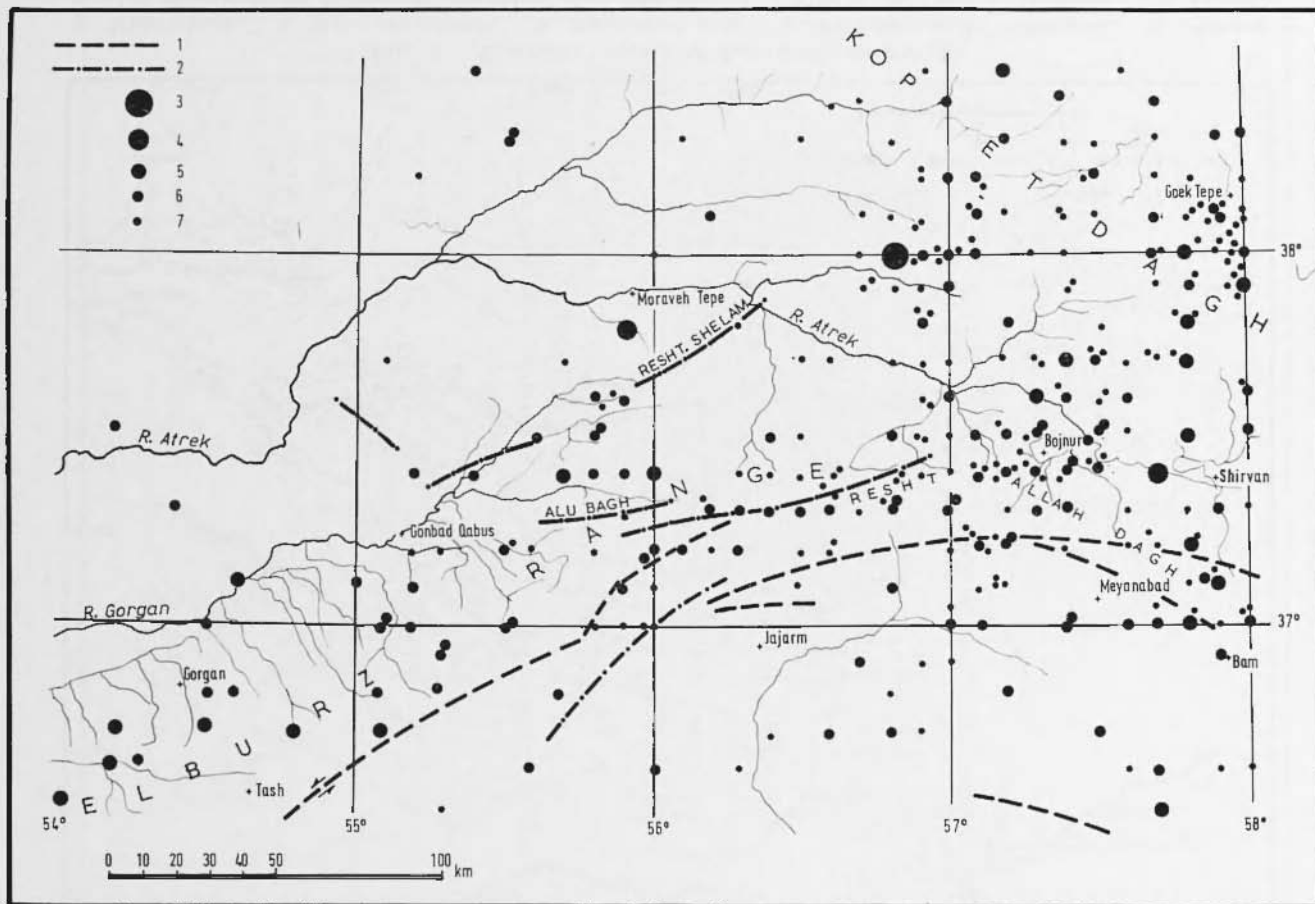


Fig. 3 - Distribution of epicentres for the period 1910-1970. Inset Figure 4.

1: Major fault lineaments based on NIOC - 2: Faults given by Wellman, 1965 - 3: $M > 7$ - 4: $6.0 \leq M < 7.0$. -
 5: $5.0 \leq M < 6.0$ - 6: $4.0 \leq M < 5.0$. - 7: $M < 4.0$.

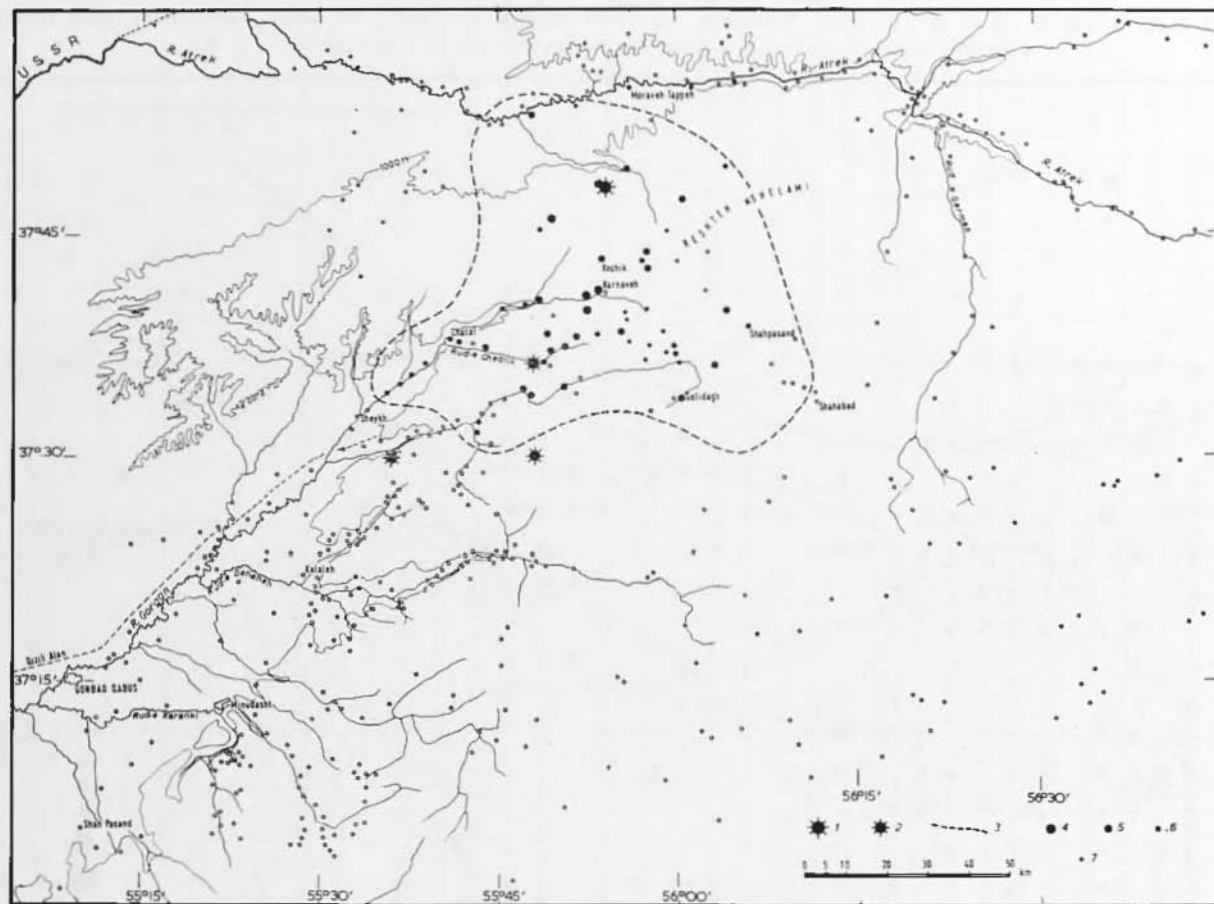


Fig. 4 - Epicentral region of Karnaveh earthquake.

1: Main shock. 2: Main aftershocks. 3: Epicentral area. 4: Villages totally destroyed. 5: Villages heavily damaged. 6: Villages that suffered some damage. 7: Other villages and settlements in the region.

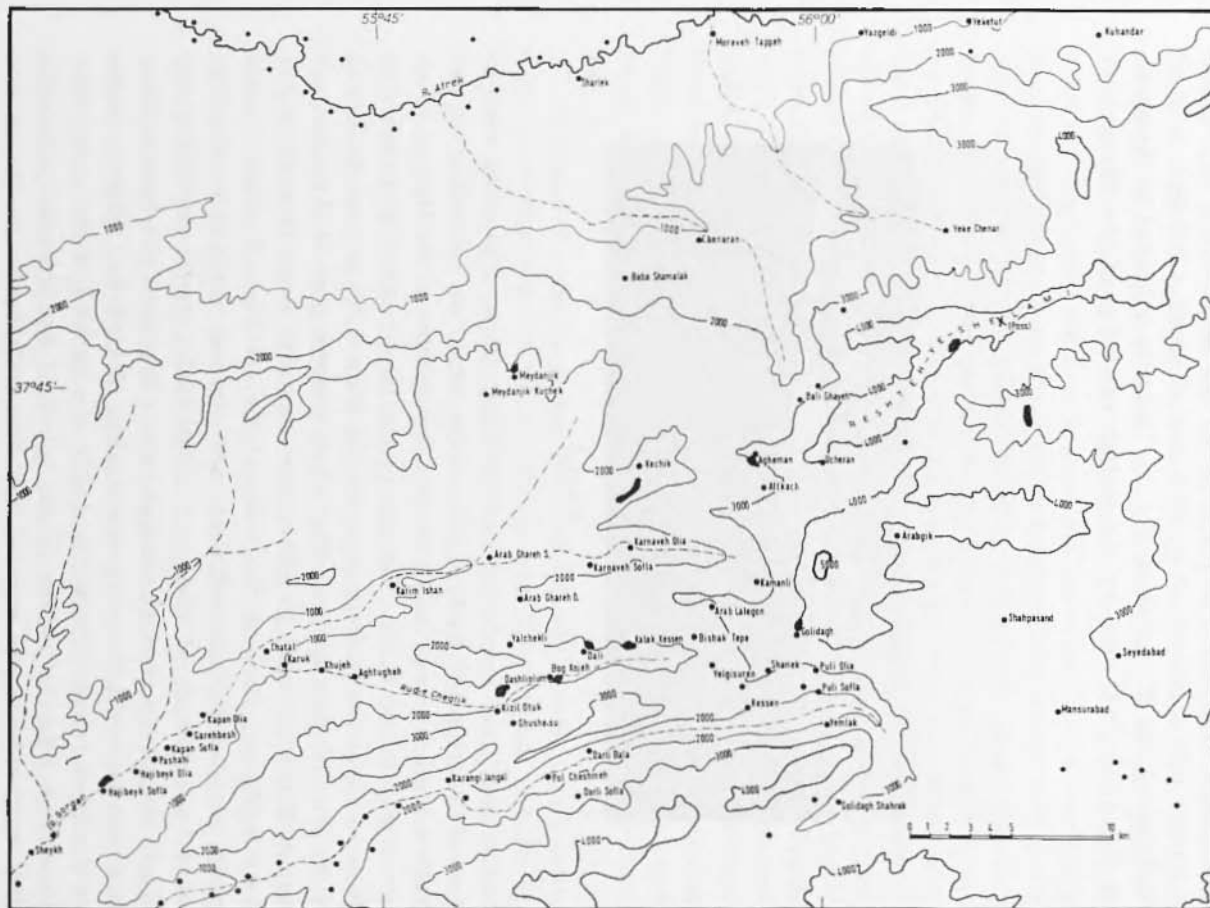


Fig. 5 - Epicentral region of Karnaveh earthquake showing all inhabited villages affected by the earthquake. Shaded areas show location of slide areas.

from the Caspian Sea, bounded on the south by the abrupt scarps of the Elburz range and on the north by the Atrek river. To the east it merges into a plateau at an elevation of about 4,000 feet, west of Shahpasand and Mansurabad, Fig. 5. This area is limited to the south by the Allah Dagh and by the eastern extension of the Elburz and



Plate I

to the east by the lower ranges of the Kopet Dagh. The entire western part of the area and parts of the eastern limits are covered to an unknown depth by loess, which in the lower reaches of the Gorgan River are over 200 feet thick. The age of the loess is from Pleistocene to Recent. Near the western edge, marine terrace deposits mark ancient shore lines of the Caspian. The whole western part of the area was apparently submerged in Pleistocene time but from then on it has been uplifting. Beneath the loess, at the eastern end of the Gorgan plain, marine Pliocene sediments are exposed, perhaps of the Tertiary transgression of the sea. These beds overlie unconformably Upper Cretaceous marine sediments which in places have been uplifted in a succession of terraces up to elevations of 4,000 feet, Plate I. Some of the more recent terracing is due to the incision of the rivers that have eroded narrow valleys in the top loess and Pliocene sediments. The only older rocks exposed are Permo-Carboniferous limestones.

Because of the absence of geological mapping of the area, and also because of the extensive Pliocene and Recent sediment cover, the geological structure of the region remains to be studied. However,

the structural units of northeastern Iran, with the Kopet Dagh and the Elburz Ranges and the recent depression of the Caspian, the Kavir-e-Damghan and the Atrek-Kashaf trough, indicate a tectonic complexity much greater than the surface geology would suggest.

The area affected by the earthquake of July 1970 is wedged between the northwest-southeast ranges of the Kopet Dagh (including its southeastern extensions into Gulul Dagh, Allahu Akbar and Hazar Masjid) and the Elburz Range (including Allah Dagh, Kuh-i Binalud, Pusht-i Kuh), the latter range starting as an east-west feature in the west but gradually curving into the Kopet Dagh direction in the east. East of Bojnurd, the Kopet Dagh and the Elburz ranges seem to merge into one unit, the axis of which is in the northwest-southeast recent and narrow trough occupied by the Atrek River running northwest and by the Kashaf River running southeast. West and northwest of Bojnurd, in the Karnaveh earthquake area, a minor structural trend, seen for example in the Rasht-e Shelami ridge, is oriented west-southwest suggesting an imbrication of the Elburz with the Kopet Dagh main structure. The geological map of Iran (17) shows three small faults in this direction within or near to the epicentral area, Fig. 3.

Wellman (22) has suggested the presence of a major active fault zone, the "Shahrud Fault", extending from the Afghan frontier to the Central Elburz, passing near Mashad, Bojnurd, Damghan, Tehran. But no such large regional and continuous fault zone was found on the ground, either in the Elburz or in the Kopet Dagh Ranges. Whereas the central Elburz mountains are bordered both to the north and along part of their southern topographical limit by large overthrust faults, these structures seem to lose their continuity east of an imaginary Gorgan-Damghan line. The Mashad-Quchan-Bojnurd recent trough in which flow the upper Atrek and Kashaf rivers is in all likelihood a major tectonic division, but available geological maps do not indicate any faults visible at the surface. Similarly, the Kopet Dagh northern border fault, which passes through Ashkhabad, does not show any pronounced surface trace even though the indirect evidence is detailed enough to inform us of its precise position (18), particularly as depicted by the ground deformations and aftershock activity associated with the Ashkhabad earthquake of 1948 (11, 19).

The damage caused by the Karnaveh earthquake followed a typical pattern met elsewhere; wherever adobe was found in the epicentral area it was totally destroyed. Thus, the fact that only this type

of construction, with its widely different inherent resistance was available for observation, made it practically impossible to assess epicentral intensities greater than about VII (MM).

In what follows we are giving a summary of the effects of the earthquake observed in the epicentral region that may facilitate future work in this part of Iran.

In Gorgan, Fig. 2, the earthquake was strongly felt but it caused absolutely no damage even to a considerable number of dilapidated houses in the central part of the town. From Gorgan, on either side of the road to Shah Pasand, a number of villages in the valley showed no sign of damage. At Shah Pasand, the shock caused some panic but no serious damage. In a few badly built houses, new cracks appeared in walls and some plaster fell off ceilings. The shock, which was accompanied by noise, caused water in small reservoirs to slosh violently.

From Shah Pasand, the road to the north leads to Gonbad Qabus, Fig. 3, a modern town built two kilometres northeast of the ruins of the early city of Jurjan, about 40 metres above the level of the Caspian Sea. In Gonbad almost all houses showed new cracks in the plaster of walls and ceilings, but with the exception of a 2-metre high, free-standing wall which before the earthquake had been condemned as being unsafe and which was thrown down, nothing else collapsed. At the entrance to the town, seven 30-metre high chimney stacks of the local brick kilns were undamaged. Also, the tomb of Ziyadi Qabus, a 51-metre high structure built early in the 11th century, was left intact. The damage caused in Gonbad was insignificant; even a small number of private houses condemned by the town engineer as unsafe for occupation were not thrown down. Again here, the ground movements caused water to be thrown out of small reservoirs and basins.

No damage was noticeable in the densely settled part of the valley between Gonbad Qabus and Minudasht. From Minudasht the road follows the foothills of the mountains that border the Gorgan plain to the east and it is level throughout. At Golikesh, a small village at the edge of Rud-e-Tarkowlu, a number of houses situated near the marshes were badly damaged. Further north, the road crosses the river Dehaneh, which at Kalaleh joins the Rud-e-Madarsu. The damage at Kalale was small but widespread, but the ground movements during the earthquake should have been rather severe as people found it difficult to walk and water was thrown out of a

small cistern measuring 2.0 by 1.0 metre in plan and 1.5 metres deep.

From Kalaleh the road follows the plain, rising gradually as it approaches the river Gorgan, which it crosses at an elevation of about 500 feet. At this point the road passes through a wide gap in "Alexander's Wall", known as the Qizil Alan, which appears as a low regular ridge, a few feet high, and which can be followed all the way to the Caspian for a distance of almost 100 kilometres. The road here enters the upper Gorgan valley. The land on each side of the valley is low, and bounded by steep sides incised by the river into the higher plateaus. From this point onwards, villages are small, scattered thinly along the narrow valleys in locations most readily irrigated, and in the winter some of the villages are only partly occupied.

At the small settlement of Sheykh, Fig. 5, the damage was serious, but only after the village of Hajibeyk did the damage become widespread. Here, almost all houses were shattered, some of them beyond repair, and during the earthquake people standing were almost thrown down. Further along the valley, Pashahi was also damaged. From this point all villages to the east are built entirely of mud without any kind of framework. At Kapan Sofla a number of houses had collapsed completely without casualties.

From Kapan Olia the road crosses a number of times the Gorgan stream or it follows the dry part of its bed. The valley becomes narrower with very steep, in places almost vertical, banks, which had slid and blocked the track with large blocks or slabs of hard loess. Just before reaching Chatal, the road which is now almost a narrow track, crosses Rud-e Cheqlik. From Chatal, a small village surrounded by a wall in places breached, the road ascends gradually following the course of the Gorgan river. The valley here becomes extremely narrow and deep, and had been blocked by landslides for many hundreds of metres which at the time of our visit, about two weeks after the event, already were eroded by the river. The damage at Chatal was considerable and, as a result of the earthquake, water from the spring had increased two-fold.

The village of Karim Ishdean was badly damaged but no houses collapsed completely. Nearby, the Medresch Elmiyeh Karim Ishan, a complex of buildings built of kiln-bricks with arched roofs surrounded by a high wall, suffered some damage. Four out of the six slender minarets decorating the Medreseh collapsed and the walls of the first floor were shattered. An inscription above the main gate indicates

that the Medreseh was built in the last decade of the 19th century which shows that the road must have been considerably used at one period.

Following the river the track climbs up gradually towards the level of the higher terraces which flank the valley on both sides reaching an altitude of 1,500 feet. The village of Arab Ghareh was heavily damaged and a number of houses had collapsed. At this point the track stops and one has to follow the river bed of Gorgan which leads to Karnaveh Sofla. In this village almost all the houses were destroyed or damaged beyond repair and 45 out of the 490 inhabitants of the village were killed. The Mosque and the Medreseh Elmiyeh, built of kiln-bricks, were damaged beyond repair; a considerable part of the Caravanserai was ruined and the school was totally destroyed. In contrast, a few barns on wooden stilts were not thrown down. Numerous slides had fallen on the village from the north face of the cliffs causing additional damage. The shock is described as having lasted a long time, causing progressive damage to the houses, but it was not strong enough to throw down standing people. The flow of the Gorgan stream, which passes through the village, had increased after the earthquake.

Karnaveh Olia, a smaller village, was also damaged, and a number of mud huts collapsed killing 12 out of 360 inhabitants of the village. Landslides and slumping of the ground near the river were responsible for some of the damage, Plate II.

From this place the track turns south and climbs up to the elevation of the main plateau at about 3,000 feet; it skirts Kamanli which was almost totally ruined and descends towards Yemlak after passing near Golidagh where landslides and slumping of the ground caused serious damage, Plate III. The twin settlement of Puli is located in densely wooded country and in both villages houses are of timber-framed construction. In contrast with other villages to the north, the damage at Puli was very small. The track ascends again towards the plateau which it reaches at Gholidagh Shahrak, a modern village with a population of 700. The damage here was considerable and about 25 people were killed, mainly in the ruins of mud huts. Better built houses of kiln-brick construction with light roofs of galvanised sheets, suffered little damage. The ground movements at Gholidagh lasted about 15 seconds and were not very strong: they caused water to slosh in cisterns and to be thrown out of small reservoirs, mainly to the west. The region south of Gholidagh for at least 45 kilometres is uninhabited.

The damage in the Rud-e-Cheqlik valley was considerable, particularly at Aghtugheh where a number of people were killed. At Kizil Otuk and at Ghushe-su almost all the mud-huts were damaged



Plate II



Plate III

or destroyed and a small number of people perished in the ruins. Large landslides and slumping of terraces added to the damage at Dashliolum where the track leading from Chatal to Puli was blocked. At

Bog Kojeh most of the damage was due to landslides which extend on either side of the valley to Dali and Kalak Kessen and to a lesser extent to Bishak Tepe. These slides, some of them incipient, follow the steep sides of the valley and they have produced some cracking and fissuring of the ground near the edge of the plateau, 200 to 300 feet above the floor of the valley.

From Gholidagh Shahrak a track leading to the northeast ascends to the plateau and joins a newly built road near Shahpasand, a new village which suffered very little damage; free-standing brick walls 1.50 metres high were found undamaged. In places the new road which leads to the north towards the Pass of Reshteh-ye-Salami, is on embankments which showed signs of slumping. About 10 kilometres north of Shahpasand, at a summer camp, water was thrown out of a small basin 1.50 by 0.75 metres in plan and 0.3 metres deep, mostly to the west. At this place, as well as near Mansurabad, people kneeling in prayer were thrown down by the shock which lasted between 10 and 20 seconds.

The new road crosses Reshteh-ye-Shelami at the Pass where there is ample evidence of severe shaking which, however, caused no apparent damage to a number of modern well built structures, but did cause some cracks to open in the road surface. From the Pass, Yeke Chenar can be seen in the distance with the 3,000 feet Range at the back, Plate I. The new road stops at the Pass and a track leads north through Yeke Chenar to Moraveh Tappeh on the Atrak river. The damage at Moraveh Tappeh was not serious but all houses were badly shaken and water was thrown out of ponds. People found it difficult to walk and the shock lasted about 20 seconds. With the exception of Yeketut where one house collapsed, the damage to the villages along the river Atrak was insignificant.

To the south of Moraveh Tappeh the plain is barren and almost uninhabited for at least 25 kilometres with the exception of Chenaran where the destruction was almost complete. In this village 7 people were killed and many injured. Baba Shamalak was also totally destroyed and many people were killed. Here, as well as at Meydanjik people and camels were thrown down by the shock and wooden chests were overturned. Near the edge of the stream that passes between Meydanjik Kuchek and Meydanjik the ground had slumped and the banks of the stream were flattened.

Further to the southeast Kechik was heavily damaged and a number of people were killed. Here as well as at Altkach and Agheman

the ground movements were very strong and the damage heavy. Large landslides and discontinuous fracturing of the ground, particularly near the edge of steep slopes, could be seen throughout this region.



Plate IV

Figure 4 summarizes the effects of the earthquake. For additional information, the reader is referred to reference (3).

A careful search in the epicentral region and the study of aerial photographs taken after the earthquake for some parts of the region did not disclose any trace of recent ground deformations of tectonic origin associated with the earthquake. The earthquake triggered many slides and caused intense slumping and fracturing of the ground, particularly close to the edge of steep ridges. Fig. 5 shows the location of some of the larger slides in the epicentral area.

The largest slide was found near Kechik in a narrow steep-sided valley a few kilometres long, Plate IV. At this place a stream has incised in the plateau and it has base-levelled a small valley floor some 200 feet below the level of the plateau, in places 300 to 500 feet wide. At the present time, the stream has cut into the valley floor a new bed about 30 feet wide and 10 to 20 feet deep. As a result of the earth-



Plate V

quake, the valley floor slumped and in places slid into the new bed, choking the stream, Plate V. The flow of water in the stream, which at the time of our visit was very small, was arrested and water was ponding in a number of pools formed by the closing of the bed. The scarps produced by the slumping of the valley floor are continuous for hundreds of feet and they have disrupted a track leading to Kechik in many places. A strain metre installed across one of these scarps detected a slow movement of the valley floor towards the stream of about 5 mm/week, Plate VI⁽¹⁰⁾. The total length of the scarps, produced by slumping in this valley, extends for about two kilometres, trending in a north-northeast direction.

Both macroseismic and instrumental epicentres fall within the limits of the principal mountain ranges, i.e. in the Elburz, Kopet Dagh and Allah Dagh. Many comparatively large earthquakes originate in the Elburz and in the Allah Dagh whereas the weaker shocks are for the most part concentrated in the Kopet Dagh. The larger

number of earthquakes in the Kopet Dagh region shown in Fig. 3 is merely the result of a better seismic network in Soviet Turkmania. A comparison between the data available prior to 1910 and after



Plate VI

that year shows that the most seismically active regions during the last 150 years are those connected with the Elburz range; particularly with those at the junction between the Elburz and the Kopet Dagh, i.e. with the Allah Dagh region and with its extension to the northwest along the narrow trough occupied by the upper Atrek and Kashaf rivers. In this region Palaeozoic formations of the Elburz are in contact with Mesozoic rocks of the Allah Dagh and Kopet Dagh.

The Karnaveh earthquake of 1970 occurred in a region relatively quiescent in this century, at least from the macroseismic point of view. During the last 100 years no earthquakes of significant magnitude were detected in the plateau between Reshteh-ye Allah Dagħ and Reshteh-ye Shelami, and the Karnaveh earthquake may be considered as an event associated with the northern boundaries of the Elburz, at its northern junction with the Kopet Dagħ.

The location of the instrumental epicentre agrees reasonably well with the region of most severe shaking. Estimate Intensity in the epicentral region was impossible to make because of the lack of man-made structures other than local adobe houses.

ACKNOWLEDGMENTS.

This work was carried out by a UNESCO reconnaissance mission including N.N.A., J.S.T. of Imperial College London, and A.A.M. of the Plan Organisation, Tehran. The mission was in close contact with Iranian engineers and seismologists and was the guest of the Ministry of Higher Education and Science, Tehran. Dr. G. King of the Geophysical Institute, Cambridge, and Mr. Enaytollah of the Ministry of Housing, Tehran, spent a week with the authors in the field. The writers would like to record their indebtedness to Dr. H. K. Afshar and to the United Nations' staff in Tehran for their generous co-operation and for the facilities afforded during the course of the mission. Special thanks are due to Mr. Aziz Yaghuti.

REFERENCES

- (1) 'ABD AL-RAHMAN IBN ABĪ BAKR, *Kashf as salālah 'an wasf az zalzalah*. BM. Or. 5872 MS. 23b.
- (2) ABŪ DARR AHMAD, SIBT IBN AL-AJMĪ, *Kunūz ad-dahab fī tarīkh Halab*. viii.12a.
- (3) AMBRASEYS N., TCHALENKO J., MOINFAR A., *The Karnaveh, northeast Iran earthquake of 30 July 1970; a field report*. UNESCO Reconnaissance Mission Publication, Paris, 1971.
- (4) FUCHS K., *Statistik der Erdbeben von 1865 bis 1885*. Sitzungsber. Kaiserl. Akad. Wiss. Wien, 92, pp. 480, 484, 486, 1886.
- (5) GALITZIN B. B., *Additional communication about the earthquake of the 10/23 January 1909*. Izv. Imp. Akad. Nank, 243-4, 1909.

- (6) GAVEMAN B., *Kopetdaskoe zemletrasenie 1 Mai 1929*. Meteorolog. Vestnik, 6, Ashkhabad, 1929.
- (7) GIRGIS ABŪ'L-FARAG, *Kitāb muhtaṣar tawarīh ad-duwal*, 170/261.
- (8) GIRGIS AL-MAKĪN IBN AL-ADIM, *Kitāb al-magmū al-mubārak*, ii, 11/ii, 31.
- (9) ḤAMD-ALLĀH IBN ABŪ BAKR MUSTAWFĪ, *Nuzhat al-Qulūb*. xiv, 147.
- (10) KING G., International Report. Geophysical Institute, Cambridge, 1971.
- (11) LINDEN N., SAVARENSKI E., *Seismichnost' Kopetdagdkoy zoni. Zemletrasenii v CCCP*, Moscow, pp. 259-262, 1961.
- (12) LYSAKOWSKI C., *Tremblements de terre arrive dans la Russie d'Asie et en Perse*. Bull. Soc. Astron. Franc., 20, pp. 45-49, 1906.
- (13) MACGREGOR C., *Khorassan*. Allen, 2, pp. 83-90, 1879.
- (14) NAPIER G., *Collection of journals and reports on special duty in Persia*. H.M.S. Office, London, 48-63, 292, 1876.
- (15) NATURE, London, 39, 1872.
- (16) NAZAREVSKI N. V., *Germabskoe zemletrasenie 1 Mai 1929 goda*. Byull. Mosk. Ob.-va Osh. Prirod. Otd. Geolog., 60, pp. 113-123, 1932.
- (17) NIOC, "National Iranian Oil Company Geological map of Iran 1:2,500,000" Tehran, 1959.
- (18) REZANOV I. A., *Tektonika in seismichnost Turkmeno-Khorasanskikh gorod*. Izdat. Akad. Nauka, Moscow, 1959.
- (19) RUSTANOVICH D. N., *Seismichnost territorii Turkmenskoy CCP in Ashkhabadskoe zemletrasenie 1948*. Vapros. Inzen. Seism., 12, Izd. Akad. Nauk, Moscow, 1967.
- (20) STÖCKLIN J., *Structural history and tectonics of Iran*. Bull. Amer. Assoc. Petrol. Geol., 52, 7, 1968.
- (21) SYKES P., *Ten thousand miles in Persia*. Murvey, p. 23, 1902.
- (22) WELLMAN H. W., *Active wrench faults of Iran, Afghanistan and Pakistan*. Geolog. Rundschau, 55, pp. 716-735, 1965.
- (23) YATES C., *Khorassan and Sistan*. Blackwood, pp. 176-177, 49, 183, 295, 1900.
- (24) PRESS REPORTS.